Cell Tissue Res (2011) 343:509–519
DOI 10.1007/s00441-010-1114-1

REGULAR ARTICLE

Identification and functional response of interstitial Cajal-like cells from rat mesenteric artery

Aurélie Formey · Lara Buscemi · François-Xavier Boittin · Jean-Louis Bény · Jean-Jacques Meister

Received: 27 October 2010 / Accepted: 2 December 2010 / Published online: 18 January 2011

Abstract Cells with irregular shapes, numerous long thin filaments, and morphological similarities to the gastrointestinal interstitial cells of Cajal (ICCs) have been observed in the wall of some blood vessels. These ICC-like cells (ICC-LCs) do not correspond to the other cell types present in the arterial wall: smooth muscle cells (SMCs), endothelial cells, fibroblasts, inflammatory cells, or pericytes. However, no clear physiological role has as yet been determined for ICC-LCs in the vascular wall. The aim of this study has been to identify and characterize the functional response of ICC-LCs in rat mesenteric arteries. We have observed ICC-LCs and identified them morphologically and histologically in three different environments: isolated artery, freshly dispersed cells, and primary-cultured cells from the arterial wall. Like ICCs but unlike SMCs, ICC-LCs are positively stained by methylene blue. Cells morphologically resembling methylene-blue-positive cells are also positive for the ICC and ICC-LC markers α-smooth muscle actin and desmin. Furthermore, the higher expression of vimentin in ICC-LCs compared with SMCs allows a clear discrimination between these two cell types. At the functional level, the differences observed in the variations of cytosolic free calcium concentration of freshly dispersed SMCs and ICC-LCs in response to a panel of vasoactive molecules show that ICC-LCs, unlike SMCs, do not respond to exogenous ATP and [Arginine]^8-vasopressin.

Keywords ICC-like cells · Vasculature · Mesenteric arteries · Smooth muscle cells · Rat (Wistar, male)

Introduction

More than a century ago, Santiago Ramón y Cajal described nerve-like cells located along the gastro-intestinal (GI) tract (Cajal 1889, 1892). These cells were first identified in living tissues by methylene blue staining and were called interstitial cells of Cajal (ICCs). Later on, electron microscopy (EM) allowed the examination of their subcellular structures, the close association between ICCs and nerve varicosities, and the cell-to-cell gap junction contacts with smooth muscle cells (SMCs; Rogers and Burnstock 1966a, 1966b). Two types of ICCs were described in the GI tract wall: multipolar ICCs with triangular or stellate-shaped cell bodies in the myenteric plexus region and spindle-shaped intramuscular ICCs along the circular and longitudinal muscle layer.

ICCs share some characteristics with SMCs: contractile filaments, caveolae, and the expression of many membrane ion channels. However, they present several important differences from SMCs: ICCs possess numerous long thin filaments, are unable to contract in response to the activation of vasoactive receptors, and express the proto-oncogene c-kit (Torihashi et al. 1999). Gastrointestinal ICCs are divided into several subpopulations participating in three well-accepted functions: as pacemakers initiating the propagation of the electrical slow wave, as neuromodulators mediating signals from the enteric nervous system to SMCs, and as mechanoreceptors (Sanders and Ward 2006).

This work was supported by the Swiss National Science Foundation (grants FN 310000-114097 and 310300-127122).

A. Formey (✉) · L. Buscemi · J.-L. Bény · J.-J. Meister
Laboratory of Cell Biophysics, Ecole Polytechnique Fédérale de Lausanne (EPFL),
CH 1015 Lausanne, Switzerland
e-mail: aurelie.formey@epfl.ch

F.-X. Boittin
Department of Zoology and Animal Biology,
University of Geneva,
Geneva, Switzerland

Cells with irregular bodies, numerous thin long filaments, and morphological similarities to the ICCs have been found outside the GI tract, viz., in the urethra (Sergeant et al. 2000) and in the bladder (Hashitani and Suzuki 2004; Hashitani et al. 2004). These cells have been called ICC-like cells (ICC-LCs) or, more recently, interstitial cells (ICs; Pucovsky 2010). ICC-LCs have also been identified among the cardiovascular system, viz., in rabbit portal vein (Povstyan et al. 2003), guinea pig mesenteric artery (Pucovsky et al. 2003, 2007), human aorta, and carotid artery (Bobryshev 2005).

In the vascular system, ICC-LCs do not correspond to any of the other cell types present in the arterial wall: endothelial cells, smooth muscle cells (SMCs), fibroblasts, inflammatory cells, and pericytes. They morphologically resemble ICCs with their long thin filaments, the diversity of their cell shapes, and their histochemical profile, with c-kit and methylene blue positivity depending of the organs and species (Pucovsky 2010). Functionally, ICC-LCs have been shown to present, in some cases, spontaneous calcium sparks and are slightly or not contractile. Transmission EM of guinea pig mesenteric artery has shown the presence of cells with thin filaments located not only on the internal elastic lamina, immediately under the endothelium, but also on the adventitial side and deeper in the tunica media of the vessel (Pucovsky et al. 2003).

Our aim was to look for the presence of ICC-LCs in the arterial wall of rat mesenteric arteries and to characterize them. We used two criteria, viz., methylene blue staining and morphological characteristics in three experimental environments: isolated artery, freshly dispersed cells, and primary-cultured cells from the arterial wall. To characterize ICC-LCs of rat mesenteric artery further, we analyzed the variations of the intracellular free calcium concentration in response to the application of exogenous vasoactive agonists to freshly dispersed ICC-LCs and compared them with SMCs.

Materials and methods

Preparation of arteries

Male Wistar rats (300±50 g) were anesthetized with isoflurane (4%) and then decapitated in accordance with the care of animals (as edited by the Swiss Academy of Medical Sciences and the Helvetic Society of Natural Sciences). All experiments performed on rat mesenteric arteries were performed with the approval of the Cantonal Veterinary Office (authorization no. 1799.1) in agreement with the law on animal protection in Switzerland. The mesenteric vascular bed and the intestines were dissected. Rat mesenteric arteries were denuded from surrounding connective tissues and perfused with isolation solution (13.7 mM NaCl, 0.54 mM KCl, 0.04 mM KH_2PO_4, 0.04 mM NaH_2PO_4, 0.2 mM $MgCl_2$, 0.42 mM $NaHCO_3$, 0.02 mM $CaCl_2$, 0.005 mM EGTA, 1 mM HEPES, 11.1 mM glucose) in order to remove the blood trapped within the vessels.

Preparation of freshly dispersed cells

The arteries were cut into small pieces and incubated with isolation solution containing collagenase type IA-S (2 mg/ml; C5894, Sigma) and elastase type IV (1 mg/ml; E0258, Sigma) for 20 min at 37°C in order to digest the adventitia. Then, the artery samples were washed with enzyme-free isolation solution. To enrich the freshly dispersed cells preparations with ICC-LCs, the first layers of the media were mechanically dissociated with a wide-bore Pasteur pipette under a microscope. ICC-LCs could be seen under brightfield microscopy during the dissociation process. The remaining arterial tissue was removed from the solution with dissection tweezers. Next, the enzyme-free isolation solution containing the freshly dispersed cells was centrifuged for 5 min at 3000 rpm, and the pellet was resuspended in Krebs Ringer solution (145 mM NaCl, 5 mM KCl, 1 mM $CaCl_2$, 0.5 mM $MgSO_4$, 1 mM NaH_2PO_4, 20 mM HEPES, 10 mM glucose, pH 7.4). Cells were allowed to attach to treated μ-Dish$^{35mm,\ low}$ Grid-500 from ibidi for 1 h prior to calcium probe loading.

Preparation of primary-cultured cells

We followed the protocol described above for dissection and enzymatic digestion to prepare the arteries, remove the adventitia, and access the media cell layers. After being washed with enzyme-free isolation solution, the pieces of arteries were transferred to several treated μ-Dish$^{35mm,\ low}$ from ibidi (three to five arteries per dish). After a few minutes, the arteries had stuck securely enough to the dish, and 1 ml culture medium (Dulbecco's modified Eagle's medium; DMEM, Invitrogen, Basel, Switzerland) supplemented with 10% fetal calf serum (FCS; BioConcept, Allschwil, Switzerland), 20 mM L-glutamine, and 1000 U/ml penicillin/streptomycin (Invitrogen) was carefully added drop by drop into each dish.

After a few hours, the SMCs migrated outside the explants and began to divide, colonizing the dish. Culture medium was refreshed every 2 to 3 days. All experiments were performed 4-6 days after seeding.

Methylene blue staining

Krebs Ringer solution (for freshly dispersed cells and arteries) or culture medium (for primary-cultured cells) was substituted by either Krebs Ringer solution or culture

medium containing 50 μM methylene blue (M9140 Sigma). Arteries, freshly dispersed cells, and primary-cultured cells were exposed to methylene blue for 40 min at 37°C in the dark and then washed in Krebs Ringer solution or culture medium prior to observation. Methylene blue images were obtained on an upright microscope (Zeiss Axioplan), and images were acquired with a Zeiss AxioCam HRm Rev.2 camera (High range monochrome) and relevant software (Zeiss Axiovision V4.2).

As methylene blue staining directly applied to freshly dispersed cells was too weak to be significant, as mentioned in previous publications (Langton et al. 1989; Povstyan et al. 2003; Sergeant et al. 2000), the staining was applied directly to the tissue before dispersion. Experiments involving the dispersion of cells from the methylene-blue-loaded arteries were carried out as follows. Loaded arteries were cut into small pieces and digested with isolation solution containing collagenase and elastase for 20 min at 37°C in order to digest the adventitia and access the cells, which remained blue. Then, the arteries were transferred into Krebs Ringer solution containing a drop of methylene blue to avoid its release from the stained cells and mechanically dissociated under a microscope (Olympus CKX41) equipped with a color camera (Leica DFC290).

Immunohistochemistry of freshly dispersed and primary-cultured cells

The cells were fixed with 3% paraformaldehyde solution in phosphate-buffered saline (PBS) at room temperature for 10 min, washed with PBS, permeabilized with PBS containing 0.2% Triton X-100 (TX) for 5 min, washed with PBS/0.02% TX, and incubated with primary antibodies in PBS containing 0.02% TX for 1 h at room temperature. After this step, cells were washed with PBS/0.02% TX and incubated with secondary antibodies conjugated with fluorescent probes in PBS/0.02% TX for 1 h at room temperature. Preparations were washed with PBS/0.02% TX and then with water and mounted in PVA.

For vimentin staining, freshly dispersed cells were allowed to attach to the culture dishes in enzyme-free isolation solution. This resulted in limited cell attachment because of the low calcium concentration. Indeed, these attached cells were more relaxed compared with those attached in Krebs Ringer solution. The attached cells were quickly fixed and subsequently stained.

Immunohistochemistry of whole-mount rat mesenteric arteries

Arteries were fixed in acetone (100%) for 30 min at 4°C, washed in PBS, and then blocked for 1 h in PBS/1% bovine serum albumin (BSA)/0.3% Tx-100. Primary antibody incubation was performed overnight at 4°C under agitation in PBS/1% BSA/0.3% Tx-100. After being washed in PBS/1% BSA/0.3% Tx-100, the arteries were incubated for 1 h 30 min at room temperature with secondary antibody in PBS/1% BSA/0.3% Tx-100. They were washed in PBS/1% BSA/0.3% Tx-100 and stained with 4,6-diamidino-2-phenylindole (DAPI). Preparations were washed and mounted in PBS/glycerol.

Primary antibodies used were: anti-α-smooth muscle actin (SMA; SM-1, mouse [m]; IgG2a; dilution 1:50; SMA Cy3, m; Sigma C6198; dilution 1:300); anti-desmin (m, IgG1; D33; Dako M0760; dilution 1:20); anti-vimentin (m, IgG1; clone V9; Dako M0725; dilution 1:4000; chicken; LuBioScience; dilution 1:500); anti CD117 (m, IgG1; Zymed; dilution 1:100). Nuclei were stained with DAPI (Fluka, Buchs, Switzerland; dilution 1:50).

Secondary antibodies used were: anti m-IgG2a-fluorescein isothiocyanate (FITC; Molecular Probe; Southern 1080-02; dilution 1:100); anti m-IgG2a-tetramethylrhodamine isothiocyanate (TRITC; Molecular Probe; Southern 1080-03; dilution 1:100); anti-m-IgG1-TRITC (Southern 1070-03, dilution 1:100); anti-m-IgG1-FITC (Molecular Probe; Southern 1070-02, dilution 1:100); anti-chicken IgG Al.647 (Invitrogen; dilution 1:300); anti-mouse IgG Al.568 (Invitrogen; dilution 1:1000).

Negative controls in all immunostaining experiments consisted of omission of the primary antibodies.

Calcium imaging

Freshly dispersed cells were loaded with 5 μM Fluo-4 AM (acetoxymethylester form of Fluo-4; Molecular Probes; F-14201) for 30 min in Krebs Ringer solution. After being loaded, the cells were washed and incubated for 20 min with Krebs Ringer solution to allow desesterification of the Fluo-4 AM. Experiments were performed at room temperature for 3 min. After 30 s of acquisition, cells were stimulated with vasoactive substances: ATP (adenosine 5′-triphosphate disodium salt; Sigma; A3377), AVP ([Arg^8]-vasopressin; Sigma; V0377), noradrenalin (L-(-)-noradrenalin (+)-bitartrate salt monohydrate; Sigma; A9512), serotonin (serotonin hydrochloride; Sigma; H9523), angiotensin II (Calbiochem; 05-23-0101), endothelin 1 (Sigma; E7764), or potassium chloride (Sigma; P4504). Calcium measurements were performed by using an inverted confocal microscope (Olympus IX 81, Spinning Disk, Perkin Elmer), and images were acquired every 0.2 s to 0.5 s with an intensified charge-coupled device (CCD) camera (Hamamatsu EMCCD C 9100B/W). The molecules of Fluo-4 AM were excited (488 nm) by using an Argon Ion laser, and the fluorescence emitted by the cells was band-passed filtered at around 525 nm. Changes in cytosolic free calcium concentration over time were presented as the relative fluorescence intensity

change, which was calculated by dividing all images from the time series by the first image (F/F_0). The change in cytosolic free calcium concentration was measured by taking the average fluorescence intensity throughout the cell. Ultra View ERS software (Perkin Elmer) was used to record the data, which were analyzed with Metamorph software.

Statistics

Data are reported as the mean±SE of the mean (SEM); *n* indicates the number of independent experiments. Comparisons of means between groups were performed by an unpaired Student's *t*-test. $P<0.05$ was considered as a statistically significant difference.

Results

Morphological identification of ICC-LCs

ICC-LCs were observed among the freshly dispersed SMCs from rat mesenteric arteries thanks to their particular shape of irregular bodies and long thin filaments compared with the partially contracted SMCs, which presented smooth oval bodies (Fig. 1a). This partial contraction of the SMCs was attributable to the presence of calcium in the Krebs Ringer solution.

Cell enrichment

In order to facilitate their study, freshly dispersed ICC-LCs were enriched by mechanically dissociating only the first cell layers of the media. Indeed, before enrichment, few cells with an ICC-LCs morphology could be observed among our cell preparations. After enrichment, 21±5% (nine preparations from three animals) of the observed dispersed cells were ICC-LCs. ICC-LCs were identified on the basis of two criteria: morphology and positivity for methylene blue vital staining (Fig. 2).

Methylene blue positivity

Similar to ICCs, but unlike SMCs, ICC-LCs from the rat mesenteric artery were stained by methylene blue (Fig. 2a). In contrast to tissue staining, freshly dispersed cells presented weak staining for methylene blue. However, we developed a procedure to link the positive blue cells among the arteries and the freshly dispersed cells. Following the enzymatic dispersion of methylene-blue-loaded arteries, we showed that the arterial methylene-blue-positive cells occurred among the freshly dispersed cells (Fig. 2b). Even if the cells lost this staining within a few minutes, all the freshly dispersed cells that were blue had a morphology similar to ICC-LCs, as they possessed numerous filaments (Fig. 2b). Moreover, methylene blue staining of primary-cultured cells (Fig. 2c) revealed the presence of positive cells with filaments, in and around the explants.

Immunohistochemical characterization of ICC-LCs

ICC-LCs were positive for α-SMA and desmin (Fig.1b). Moreover, staining for vimentin revealed that ICC-LCs expressed more vimentin than SMCs in the three environments (Fig. 3). Double-staining of vimentin with α-SMA allowed the visualization of ICC-LCs in whole-mount arteries (Fig. 3a, b) at the external side of the media, just above the SMCs. When freshly dispersed cells were stained with anti-vimentin antibody and observed by confocal microscopy, relaxed SMCs (Fig. 3f) were almost invisible, whereas ICC-LCs (Fig. 3d) and endothelial cells (ECs; Fig. 3h) were clearly seen. As expected and unlike SMCs (Fig. 3e) and ICC-LCs (Fig. 3c), ECs (Fig. 3g) were not

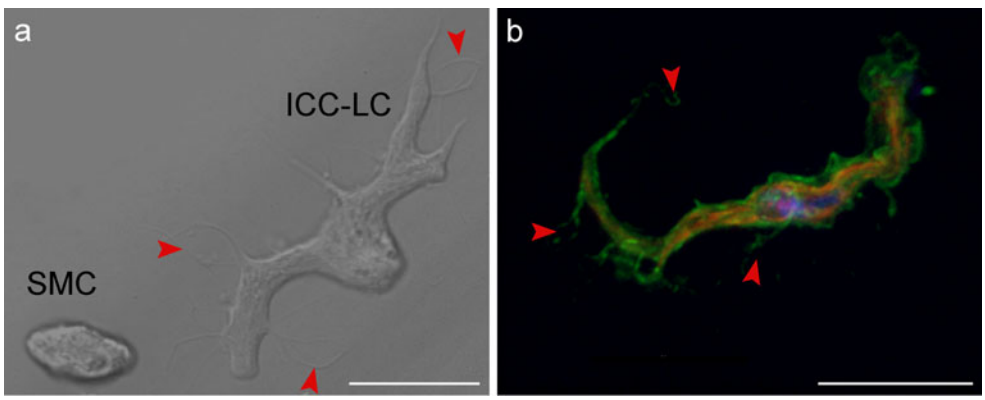

Fig. 1 Morphological identification of freshly dispersed cells from rat mesenteric artery. **a** Differential interference contrast image of an interstitial cell of Cajal (ICC)-like cell (*ICC-LC*) and a smooth muscle cell (*SMC*). **b** Cells with characteristic filaments (*arrowheads* in **a**, **b**) were positive for the ICC and ICC-LC markers α-smooth muscle actin (SMA; *green*) and desmin (*red*). The nucleus was revealed by 4,6-diamidino-2-phenylindole (DAPI) staining (*blue*). *Bars* 20 μm

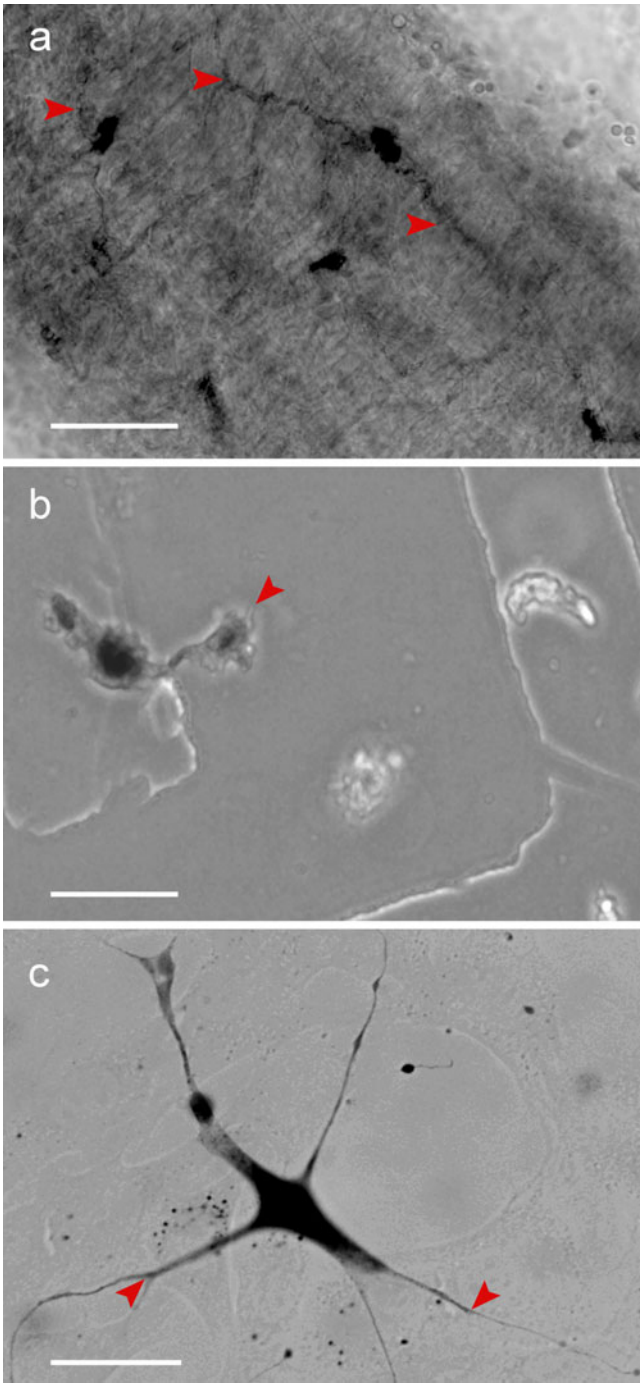

Fig. 2 Vital methylene blue staining. Positive blue cells with long thin filaments (*arrowheads*) were located among the adventitial side of the media on arteries (**a**). The methylene-blue-positive cells that were stained in the arteries before dispersion were found among the freshly dispersed cells, and all freshly dispersed cells that were blue were morphologically similar to ICC-LCs, as they presented numerous filaments (**b**, *arrowhead*). Positive cells with filaments were also found in primary cultures (**c**, *arrowheads*). Part of the grid printed on the bottom of the dish is visible in **b**. *Bars* 20 μm

positive for α-SMA staining. Primary-cultured cells with an ICC-LC morphology were also observed to express vimentin strongly within their fibers (Fig. 3j). These cells were also positive for α-SMA but were less strongly stained compared with the surrounding SMCs (Fig. 3i).

No immunoreactivity for c-kit receptors (CD117) on freshly dispersed cells was observed. Nevertheless, staining on whole-mount rat mesenteric artery revealed positive cells located in close apposition with the external medial layer of SMCs (Fig. 4b, e). These positive cells were also positive for α-SMA (Fig. 4a) and vimentin (Fig. 4d) and were organized as a small network of branching cells varying in cell shape and size like the freshly dispersed ICC-LCs.

Contraction assays

Both SMCs (n=28 cells) and ICC-LCs (n=26 cells) contracted in response to 100 mM potassium chloride (KCl) depolarization (Fig. 5). This contraction, as measured by the percentage of the original length of the cells, was statistically significant (P<0.05). Before KCl stimulation, SMCs had partially contracted because of the calcium present in the physiological Krebs Ringer solution. Nevertheless, SMC contraction in response to depolarization was significantly greater than that of ICC-LCs.

Free calcium concentration responses of freshly dispersed cells to agonists

Tonic response to KCl depolarization

Being able to identify the ICC-LCs clearly and to distinguish them from SMCs, we proceeded to study the variation of cytosolic free calcium concentration on freshly dispersed cells in response to several vasoactive molecules. All experiments were carried out at room temperature. Both ICC-LCs and SMCs presented a calcium increase in the cell body, and in the filaments of ICC-LCs, in response to the depolarization caused by the addition of extracellular KCl (Fig. 6). The application of 50 mM KCl showed three types of cytosolic calcium behaviors among the SMC population (Fig. 6a, n=27 cells): 73% of the studied SMCs presented a long-lasting intracellular calcium rise (Fig. 6a, top), whereas 19% presented an initial increase followed by small calcium oscillations (Fig. 6a, middle), and 8% exhibited calcium oscillations (Fig. 6a, bottom). All ICC-LCs (n=27 cells) presented a tonic phase response (Fig. 6b).

Response to stimulation by vasoactive molecules

In order to compare the cytosolic free calcium responses of both cell populations to agonists, we used a panel of

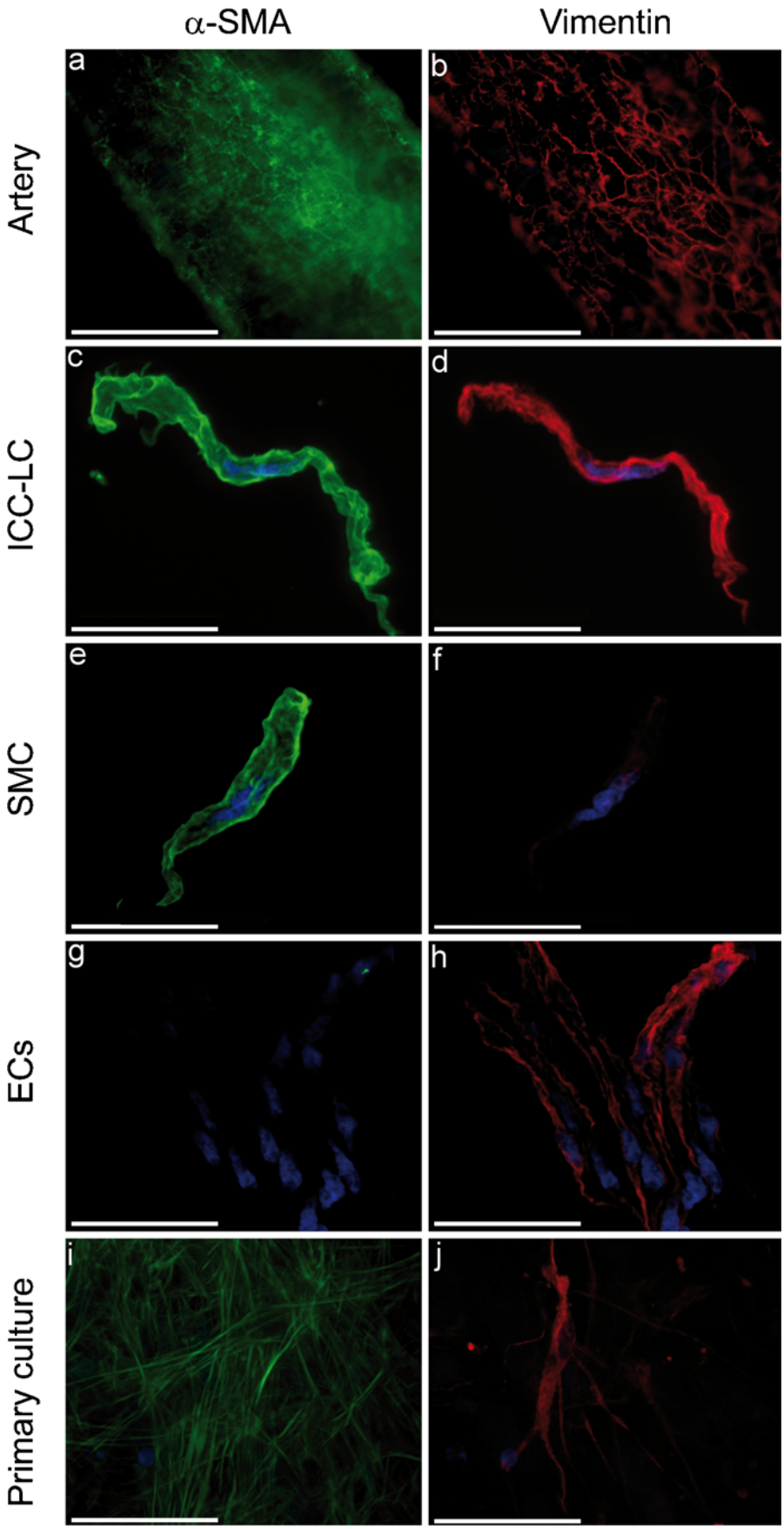

Fig. 3 Immunological properties of rat mesenteric ICC-LCs. ICC-LCs expressed more vimentin (*red*) than SMCs, and double-staining with α-SMA (*green*) allowed visualization of ICC-LCs in arteries (**a**, **b**) at the external side of the media, immediately above the SMCs. In freshly dispersed preparations (**c-h**) and in primary-cultured cells (**i**, **j**), double staining with α-SMA and vimentin allowed us to distinguish ICC-LCs from SMCs and endothelial cells (*ECs*). Nuclei were revealed by DAPI staining (*blue*). *Bars* 20 μm

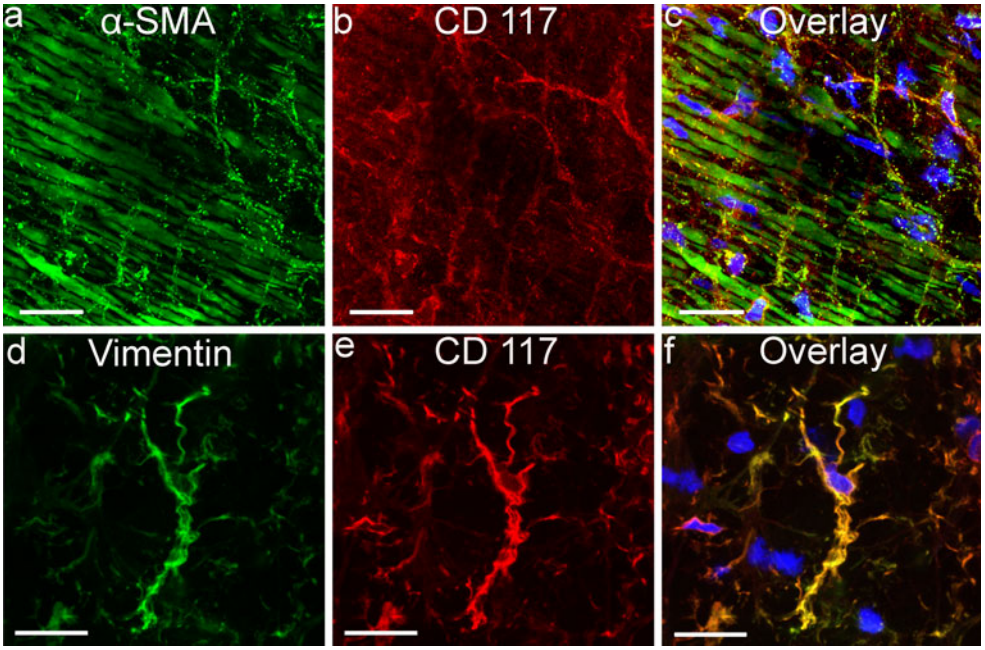

Fig. 4 Positivity of rat mesenteric arteries for c-kit receptor (CD117) staining. Cells positive for α-SMA (**a**) and vimentin (**d**) presenting long thin filaments were co-stained for c-kit receptors CD117 (**b**, **e**). Nuclei were revealed by DAPI staining (*blue*, **c**, **f**). *Bars* 20 μm

vasoactive molecules known to cause the contraction of arterial SMCs. Both SMCs and ICC-LCs presented the same pattern of calcium response to noradrenalin (10 μM), endothelin 1 (200 nM), angiotensin II (10 μM), and serotonin (100 μM). The results are summarized in Table 1. The proportion of cells responding to the aforementioned vasoactive molecules was within the same range. For each drug, the responses of both cell types were classified, at a given high concentration, in the same three categories: an immediate transient calcium rise, a calcium increase followed by oscillations, or a sustained calcium response. Figure 7 illustrates the responses to stimulation by 10 μM noradrenalin. Indeed, these experiments allowed us to highlight the ability of ICC-LCs from rat mesenteric arteries to present global cytosolic calcium oscillations in response to stimulation by vasoactive molecules: 18 out of 61 ICC-LCs (29.5%) in response to noradrenalin, three out of 43 (7%) for endothelin 1, three out of 14 (21.4%) for angiotensin II, and three out of 39 ICC-LCs (23.1%) in response to serotonin. We found that a single ICC-LC could exhibit a calcium

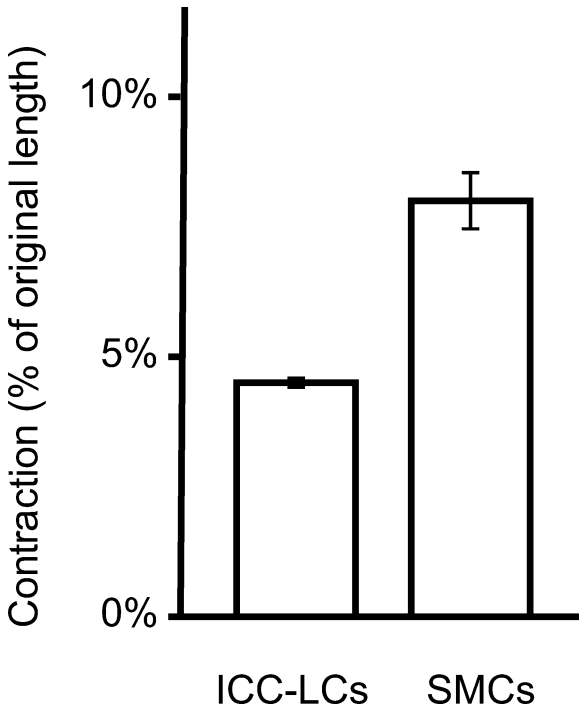

Fig. 5 Contraction of freshly dispersed ICC-LCs and SMCs in response to high potassium chloride (100 mM) depolarization. The contraction as given by the percentage of the original length of the ICC-LCs is significantly smaller ($P<0.05$) than that of SMCs

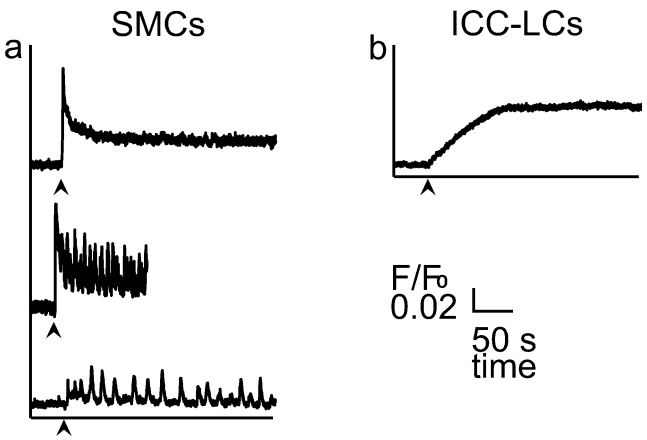

Fig. 6 Cytosolic free calcium concentration changes in response to 50 mM KCl stimulation (*arrowheads*) in SMCs (**a**) and ICC-LCs (**b**). SMCs presented three kinds of behavior in response to KCl depolarization: long-lasting (*top*, 73%), initial increase followed by small calcium oscillations (*middle*, 19%), or calcium oscillations (*bottom*, 8%); 100% of ICC-LCs present a tonic phase behavior in response to the same stimulus. F/F_0 represents the fluorescence ratio

Table 1 Percentage of cells (interstitial cells of Cajal [ICC]-like cell [*ICC-LCs*] versus smooth muscle cells [*SMC*]) responding to various drugs known to act as SMC agonists in the vasculature. ICC-LCs, unlike SMCs, did not respond to stimulation by high concentrations of adenosine 5′-triphosphate (*ATP*; 200 μM) or [Arg]^{8}-vasopressin (*AVP*; 500 nM)

Cell type	Noradrenalin (10 μM)	Endothelin 1 (200 nM)	Angiotensin II (10 μM)	Serotonin (100 μM)	ATP (200 μM)	AVP (500 nM)
ICC- LCs	55.36% *n*=112	60.56% *n*=71	32.56% *n*=43	37.5% *n*=104	5.55% *n*=18	0% *n*=22
SMCs	40.44% *n*=272	50.78% *n*=128	36.84% *n*=76	28.05 *n*=246	100% *n*=77	100% *n*=48

response to one or several vasoactive molecules. Moreover, responsive ICC-LC did not necessarily exhibit the same behavior in response to those different agonists (data not shown).

Differential responses to ATP and AVP

In contrast to the results that highlighted the capacity of ICC-LCs to oscillate in response to certain stimuli, and unlike SMCs, ICC-LCs did not respond to stimulation by exogenous AVP or ATP (Fig. 8). Of the ICC-LCs, 100% (Fig. 8b) did not respond to AVP stimulation (500 nM) compared with SMCs (Fig. 8a), 22.9% of which responded with a transient calcium rise, 37.5% with calcium oscillations, and 39.6% with a sustained calcium response. In addition, in response to 200 μM ATP stimulation (Fig. 8c, d), 1.3% of SMCs responded with a transient calcium rise, 14.3% by calcium oscillations, and 84.4% by a long-lasting calcium increase. In comparison, 1 ICC-LC out of 20 responded with a transient response. Cell viability control was performed by the addition of KCl (100 mM) at the end of every calcium experiment; this showed that 100% of the cells responded to depolarization.

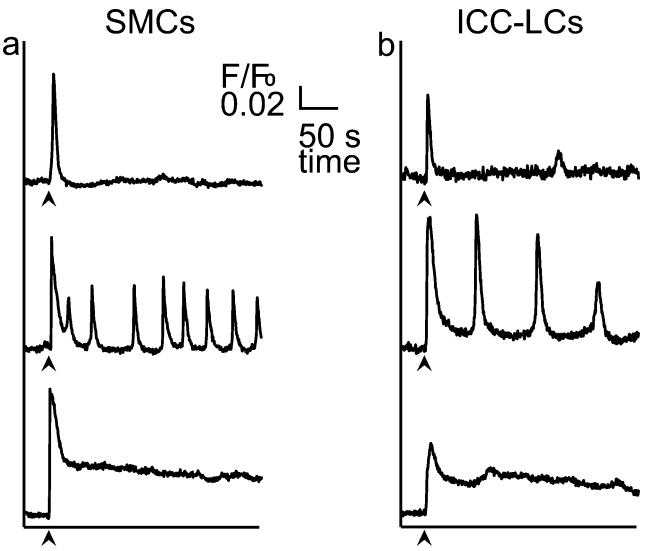

Fig. 7 Cytosolic calcium responses of freshly dispersed SMCs and ICC-LCs in response to stimulation (*arrowhead*) by 10 μM noradrenalin. Both cell types present a transient (*top*) or long-lasting (*bottom*) cytosolic calcium increase and cytosolic calcium oscillations (*middle*). F/F_0 represents the fluorescence ratio

Discussion

Characteristics of ICC-LCs of rat mesenteric artery

Methylene blue positivity

We have found ICC-LCs in rat mesenteric arteries, as shown by their morphological and immunological properties. The morphological characteristics of ICCs and ICC-LCs have been demonstrated to be species- and tissue-dependent (Burns et al. 1997; Komuro 1999; Komuro et al. 1999), but most of

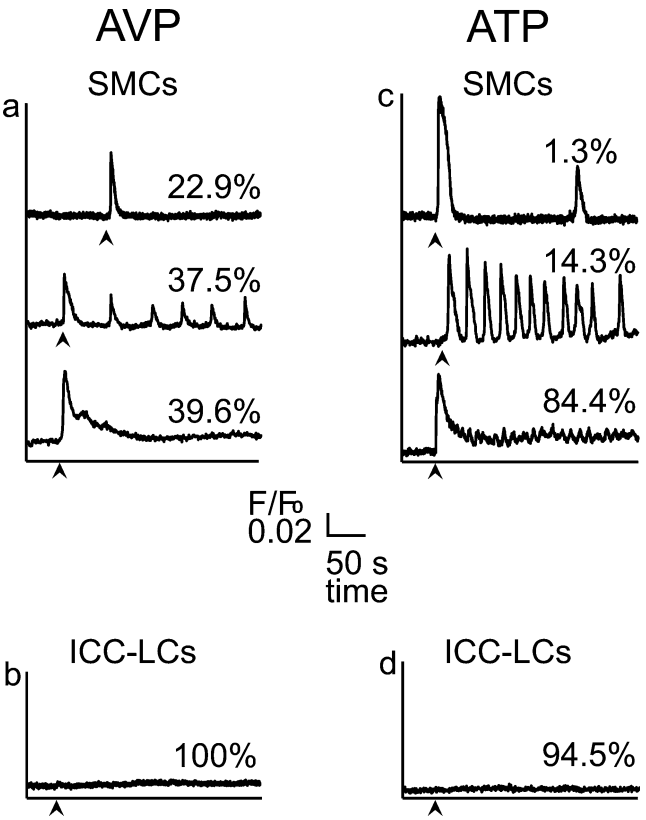

Fig. 8 Cytosolic free calcium concentration changes in response to 500 nM AVP (**a**, **b**) and 200 μM ATP (**c**, **d**) stimulation (*arrowheads*) in SMCs and ICC-LCs. SMCs presented three different behaviors in response to AVP and ATP: a transient calcium increase (*top*), cytosolic calcium oscillations (*middle*), and long-lasting calcium increase followed (or not) by small calcium oscillations (*bottom*). None of the 22 ICC-LCs responded to AVP, and 17 of the 18 studied ICC-LCs did not respond to ATP. F/F_0 represents the fluorescence ratio

the gut ICCs are readily stained by methylene blue and express vimentin and the proto-oncogene c-kit (Huizinga et al. 1995; Ward et al. 1994). In contrast to observations in guinea pig (Pucovsky et al. 2003, 2007), ICC-LCs have been positively stained with methylene blue in the rat isolated artery, in freshly dispersed cells, and in primary-cultured cells. In the artery, a dense network of positive blue ICC-LCs has been distinguished in the adventitial side of the media, compatible with the existence of pacemaking regions (Harhun et al. 2005). Despite the observations published on ICCs from GI (Epperson et al. 2000) and ICC-LCs from rabbit portal vein (Povstyan et al. 2003), we have been able to develop a method to stain single isolated ICC-LCs by methylene blue with an improved new protocol based on cell dispersion from methylene-blue-loaded arteries. Isolated ICC-LCs show a morphological diversity with filaments varying from cell to cell in terms of number, length, and thickness, as seen in other tissues (Langton et al. 1989; Povstyan et al. 2003; Sergeant et al. 2000). Such observations have also been made in single isolated ICCs from canine proximal colon (Langton et al. 1989), rabbit urethra (Sergeant et al. 2000), rabbit portal vein (Povstyan et al. 2003), and, recently, guinea pig mesenteric artery (Pucovsky and Bolton 2006). These observations suggest the existence of sub-populations of ICC-LCs exhibiting diverse functions.

Our finding that methylene-blue-positive cells are localized on the adventitial side of the media, which is densely innervated, is in accordance with other arterial ICC-LC locations:, e.g., in the tunica media of small resistance arteries (Dahl and Nelson 1964; Lee 1995; Pucovsky et al. 2003) and in human aorta and carotid artery (Bobryshev 2005) along the border between the media and adventitia where they lie in direct contact with nerve endings. Therefore, ICC-LCs might have a role as an intermediary between nerves and SMCs (Pucovsky et al. 2003).

High vimentin expression

In addition to the observation that, like GI ICCs and unlike SMCs, rat mesenteric artery ICC-LCs are positive for vital methylene blue staining, we have shown that they also express the molecular markers desmin, α-SMA, and vimentin. The positivity of ICC-LCs for α-SMA and desmin (Pucovsky et al. 2003) excludes the possibility that these cells are one of the other types of cells present in arteries such as fibroblasts, pericytes or neuronal and dendritic cells. Vimentin staining is usually used to distinguish ICCs and ICC-LCs from SMCs (Hatton et al. 2001; Rumessen 1996; Sergeant et al. 2000; Suciu et al. 2007), as the ICC-LCs exhibit higher vimentin expression, especially inside the filaments. The α-SMA expression combined with the higher vimentin expression has allowed us to differentiate them from other cell types and to localize them on the artery, among freshly dispersed cells, and among primary-cultured cells. This double-staining with vimentin and α-SMA validates our three-environment model study, as we can, after experiments on living cells, fix them and discriminate ICC-LCs from SMCs.

Proto-oncogene c-kit expression

Even if no evidence of immunoreactivity for c-kit receptors (CD117) had been found on freshly dispersed cells from rat mesenteric artery, as detected by Epperson et al. (2000) in murine small intestine, immunostaining of the whole-mount arteries has provided evidence for the existence of CD117-positive cells located in close apposition above the smooth muscle cells at the external side of the media. In addition, most of those CD117-positive cells also express either vimentin or α-SMA. C-kit receptors might also be expressed in hematopoietic stem cells, mast cells, germ cells, and melanocytes. Moreover, stem cells and mast cells might express vimentin and be present on the arterial wall. Nevertheless, as far as we know, none of these cells possess α-SMA-positive fibers or have elaborate long thin filaments.

Our study has allowed us to check for the presence of methylene-blue-positive freshly dispersed cells directly stained from the tissue. The enrichment of freshly dispersed ICC-LCs and the identification of primary-cultured ICC-LCs have enabled us to locate rat mesenteric artery ICC-LCs at three levels of organization, viz., isolated artery, freshly dispersed cells, and primary-cultured cells, thereby giving us a model in which we can work on ICC-LCs to try to elucidate their physiological role.

With a reliance only on freshly dispersed cells, many mechanistic and biochemical studies of rhythmicity, second messenger coupling, agonist effects, and cell-to-cell interactions might be difficult to pursue (Publicover et al. 1992). Data have suggested that the pacemaker function of primary-cultured ICCs is retained for several days (Thomsen et al. 1998). Therefore, primary cultures may be a good model for further studies of the rat mesenteric ICC-LC mechanisms involving the regulation of pacemaker activity. The study of primary-cultured cells might also provide advances for an understanding of cell-to-cell communication of ICC-LCs with each other and with SMCs.

ICC-LCs and SMCs can be distinguished by their responses to agonists

The characteristically tonic phase response of ICC-LCs to high KCl depolarization compared with the multiple behavioral responses by the SMCs is the first element that confirms the hypothesis that ICC-LCs and SMCs can be distinguished on a functional basis.

ICC-LC oscillatory state

A certain proportion of freshly dispersed ICC-LCs exhibit global cytosolic calcium oscillations in response to noradrenalin (29.5%), endothelin 1 (7%), angiotensin II (21.4%), and serotonin (23.1%). The ability of these cells to oscillate in response to a stimulus has shown that they possess a calcium oscillator machinery. The finding that not all ICC-LCs respond with the same behavior to the application of an exogenous molecule at a given concentration highlights their different sensitivities. These differences suggest that all ICC-LCs do not have the same toolkit of receptors or, at least, that they do not have the same sensitivities. Nevertheless, the hypothesis of the existence of several subpopulations of ICC-LCs exhibiting diverse functions, as is the case for GI ICCs, needs further investigation.

Responses to AVP and ATP

This is the first time that a physiological difference between ICC-LCs and SMCs has been revealed in the vasculature. ICC-LCs respond to some vasoactive molecules, but not to AVP and ATP. However, these molecules are present in the vascular system and produce a cytosolic calcium rise in all SMCs, leading to their contraction. Further investigations concerning the putative relationship between the signaling molecules of nerve endings and the calcium responses of ICC-LCs should be of interest for the comprehension of the role of ICC-LCs on the arterial wall. Indeed, this difference of functionality between ICC-LCs and SMCs underlines the possible different roles of these cells.

The exact functions of ICC-LCs from the rat mesenteric artery have not as yet been identified. ICC-LCs have been shown to be present in rat mesenteric arteries, and we have been able to study their responses to agonists in order to characterize them at the functional level. In addition, we have succeeded in clearly differentiating them from SMCs. This will facilitate future studies of their physiological role in the vasculature. The isolated artery allows the cells to be studied in their physiological location. We can also access the single cell level with freshly dispersed cells, and cell-to-cell interactions with primary-cultured ICC-LCs and SMCs. Based on the results of the current study, calcium imaging with a panel of vasoactive molecules appears to be a helpful tool for examining the physiology of ICC-LCs and their relationship to SMCs. Further investigations are needed to improve our understanding of the physiology and of the roles of ICC-LCs in the vasculature.

Acknowledgments We thank Juan-Carlos Sarria, Thierry Laroche, and Alessandra Griffa for expert help with the imaging experiments and data processing. We are also grateful to Nadia Halidi and François Delavy for fruitful discussions and to Josiane Smith-Clerc for excellent technical assistance.

References

Bobryshev YV (2005) Subset of cells immunopositive for neurokinin-1 receptor identified as arterial interstitial cells of Cajal in human large arteries. Cell Tissue Res 321:45–55

Burns AJ, Herbert TM, Ward SM, Sanders KM (1997) Interstitial cells of Cajal in the guinea-pig gastrointestinal tract as revealed by c-Kit immunohistochemistry. Cell Tissue Res 290:11–20

Cajal SR (1889) Nuevas aplicaciones del metodo de coloracion de Golgi. Gac Med Cat 12:613

Cajal SR (1892) El plexo de Auerbach de los batracios. Nota sobre el plexo de Auerbach de la rana. Trab Lab Histol Fac Med Barcelona (1892):23-28

Dahl E, Nelson E (1964) Electron microscopic observations on human intracranial arteries. II. Innervation. Arch Neurol 10:158–164

Epperson A, Hatton WJ, Callaghan B, Doherty P, Walker RL, Sanders KM, Ward SM, Horowitz B (2000) Molecular markers expressed in cultured and freshly isolated interstitial cells of Cajal. Am J Physiol Cell Physiol 279:C529–C539

Harhun MI, Pucovsky V, Povstyan OV, Gordienko DV, Bolton TB (2005) Interstitial cells in the vasculature. J Cell Mol Med 9:232–243

Hashitani H, Suzuki H (2004) Identification of interstitial cells of Cajal in corporal tissues of the guinea-pig penis. Br J Pharmacol 141:199–204

Hashitani H, Yanai Y, Suzuki H (2004) Role of interstitial cells and gap junctions in the transmission of spontaneous Ca^{2+} signals in detrusor smooth muscles of the guinea-pig urinary bladder. J Physiol (Lond) 559:567–581

Hatton WJ, Mason HS, Carl A, Doherty P, Latten MJ, Kenyon JL, Sanders KM, Horowitz B (2001) Functional and molecular expression of a voltage-dependent K(+) channel (Kv1.1) in interstitial cells of Cajal. J Physiol (Lond) 533:315–327

Huizinga JD, Thuneberg L, Kluppel M, Malysz J, Mikkelsen HB, Bernstein A (1995) W/kit gene required for interstitial cells of Cajal and for intestinal pacemaker activity. Nature 373:347–349

Komuro T (1999) Comparative morphology of interstitial cells of Cajal: ultrastructural characterization. Microsc Res Tech 47:267–285

Komuro T, Seki K, Horiguchi K (1999) Ultrastructural characterization of the interstitial cells of Cajal. Arch Histol Cytol 62:295–316

Langton P, Ward SM, Carl A, Norell MA, Sanders KM (1989) Spontaneous electrical activity of interstitial cells of Cajal isolated from canine proximal colon. Proc Natl Acad Sci USA 86:7280–7284

Lee RM (1995) Morphology of cerebral arteries. Pharmacol Ther 66:149–173

Povstyan OV, Gordienko DV, Harhun MI, Bolton TB (2003) Identification of interstitial cells of Cajal in the rabbit portal vein. Cell Calcium 33:223–239

Publicover NG, Horowitz NN, Sanders KM (1992) Calcium oscillations in freshly dispersed and cultured interstitial cells from canine colon. Am J Physiol 262:C589–C597

Pucovsky V (2010) Interstitial cells of blood vessels. ScientificWorldJournal 10:1152–1168

Pucovsky V, Bolton TB (2006) Localisation, function and composition of primary Ca(2+) spark discharge region in isolated smooth muscle cells from guinea-pig mesenteric arteries. Cell Calcium 39:113–129

Pucovsky V, Moss RF, Bolton TB (2003) Non-contractile cells with thin processes resembling interstitial cells of Cajal found in the wall of guinea-pig mesenteric arteries. J Physiol (Lond) 552:119–133

Pucovsky V, Harhun MI, Povstyan OV, Gordienko DV, Moss RF, Bolton TB (2007) Close relation of arterial ICC-like cells to the contractile phenotype of vascular smooth muscle cell. J Cell Mol Med 11:764–775

Rogers DC, Burnstock G (1966a) The interstitial cell and its place in the concept of the autonomic ground plexus. J Comp Neurol 126:255–284

Rogers DC, Burnstock G (1966b) Multiaxonal autonomic junctions in intestinal smooth muscle of the toad (*Bufo marinus*). J Comp Neurol 126:625–652

Rumessen JJ (1996) Ultrastructure of interstitial cells of Cajal at the colonic submuscular border in patients with ulcerative colitis. Gastroenterology 111:1447–1455

Sanders KM, Ward SM (2006) Interstitial cells of Cajal: a new perspective on smooth muscle function. J Physiol (Lond) 576:721–726

Sergeant GP, Hollywood MA, McCloskey KD, Thornbury KD, McHale NG (2000) Specialised pacemaking cells in the rabbit urethra. J Physiol (Lond) 526:359–366

Suciu L, Popescu LM, Gherghiceanu M (2007) Human placenta: de visu demonstration of interstitial Cajal-like cells. J Cell Mol Med 11:590–597

Thomsen L, Robinson TL, Lee JC, Farraway LA, Hughes MJ, Andrews DW, Huizinga JD (1998) Interstitial cells of Cajal generate a rhythmic pacemaker current. Nat Med 4:848–851

Torihashi S, Nishi K, Tokutomi Y, Nishi T, Ward S, Sanders KM (1999) Blockade of kit signaling induces transdifferentiation of interstitial cells of Cajal to a smooth muscle phenotype. Gastroenterology 117:140–148

Ward SM, Burns AJ, Torihashi S, Sanders KM (1994) Mutation of the proto-oncogene c-kit blocks development of interstitial cells and electrical rhythmicity in murine intestine. J Physiol (Lond) 480:91–97